

## Nonperturbative density functional theory of solid-to-solid isostructural transitions

This article has been downloaded from IOPscience. Please scroll down to see the full text article.

1995 J. Phys.: Condens. Matter 7 6797

(<http://iopscience.iop.org/0953-8984/7/34/005>)

View [the table of contents for this issue](#), or go to the [journal homepage](#) for more

Download details:

IP Address: 171.66.16.151

The article was downloaded on 12/05/2010 at 21:59

Please note that [terms and conditions apply](#).

# Nonperturbative density functional theory of solid-to-solid isostructural transitions

C N Likos and G Senatore

Dipartimento di Fisica Teorica, Università di Trieste, Strada Costiera 11, I-34014 Grignano (TS), Italy

Received 28 April 1995, in final form 21 June 1995

**Abstract.** We examine the phase diagram of systems of hard, spherical particles with a short-range attraction. Recent simulations as well as theoretical investigations predict for such systems an fcc-to-fcc isostructural transition which terminates at a critical point, and the existence of a single fluid phase. We use a nonperturbative density functional approach, by making a mapping of the inhomogeneous system onto a uniform fluid by means of the modified weighted density approximation (MWDA). Previous approaches were instead based on the separation of the potential into a hard-sphere repulsion and a short-range attraction with the latter treated in a mean-field fashion. We obtain improved results for the critical temperature, the middle density at the triple point and the overall shape of the phase diagram, but a worsening of the triple temperature with increasing range of interaction.

## 1. Introduction

Probably the best understood phase transition of classical fluids is the liquid–gas transition. The study of this phase change goes back to the pioneering work of van der Waals who demonstrated that there is no fundamental difference between a liquid and a gas: one phase can be continuously transformed into the other above the critical temperature  $T_c$ , and below  $T_c$  the two phases are separated by a first-order phase transition. A fundamental requirement for such a transition to take place is the existence of an attractive part in the interparticle interaction in addition to the (core) repulsion. Systems interacting by means of *purely repulsive* potentials possess a single fluid phase, coexisting at high packing with a solid whose crystalline structure (i.e. fcc, bcc etc) depends on the steepness of the repulsion.

Although necessary to cause a liquid–gas transition, the existence of an attractive part in the interparticle potential is not sufficient to produce such a phase change. Indeed, whether a given system will possess one or two fluid phases depends on the range of the attractive interaction. There is by now ample evidence for a variety of one- and two-component mixtures with a hard-core repulsion that, when the range of the attractive part becomes less than 25% of the hard-sphere diameter, the liquid–gas critical point becomes thermodynamically unstable because  $T_c$  drops below the triple temperature  $T_t$  [1, 2]. On the other hand, recent simulations by Bolhuis *et al* [2, 3] showed that if the range of the attractive potential is small enough (roughly speaking less than 7% of the hard-sphere diameter), there exist two fcc *solid* phases, separated by a line which terminates at a critical point. Solid-to-solid transitions between two solids of *different* crystal symmetry are quite common and they have been known for many years. However, this is an *isostructural* transition between two solids that differ only in their thermodynamic density (lattice constant) and in that respect

it bears a close resemblance to the liquid–vapour transition, which can be thought of as its analogue for translationally invariant phases. This remarkable discovery, found to hold for two- as well as three-dimensional systems and for square well and attractive Yukawa-tail potentials [2], establishes a symmetry in the phase diagrams of simple systems: when the range of the attractive potential is sufficiently long, the phase diagram of the system consists of a single solid phase and two fluid ones. When it is short enough, there are two solid phases and a fluid one, whereas for intermediate values of the attractive range, only a single fluid and a single crystal phase occur.

There has already been considerable theoretical effort to explain these simulation results. The qualitative characteristics of the phase diagram can readily be understood within the framework of the uncorrelated cell model [2]. Moreover, Tejero *et al* have studied the same systems by means of a variational procedure based on the Gibbs–Bogoliubov inequality [4, 5], and Daanoun *et al* have presented an analytic van der Waals-type theory for solids [6] to manifest the symmetry between the fluid and solid coexistence regions of the system. Finally, a density functional treatment of the problem has recently been proposed by Likos *et al* [7], where the interaction is split into a hard-sphere part, treated nonperturbatively using the modified weighted density approximation (MWDA) of Denton and Ashcroft [8], and an attractive part which is treated in a mean-field fashion. This separation is necessary for systems displaying a phase diagram with a two-fluid-phase region [9], where the correlation functions of the fluid are not well-defined, and the mapping of the solid onto a fluid is then problematic. However, as mentioned above, systems with a short-range attractive interaction with which we are concerned here possess a *single* fluid phase, and such a mapping is possible for the *correlation* part of the Helmholtz free energy, as we demonstrate below.

The layout of this paper is as follows: in section 2 we describe the system and its fluid state properties (correlation functions and excess free energy). In section 3 we present the method that we use to describe the solid phases of the system, and to obtain the phase diagram. In section 4 we present our results and compare them with the ones from the mean-field treatment and from simulation. Finally, in section 5 we draw our conclusions.

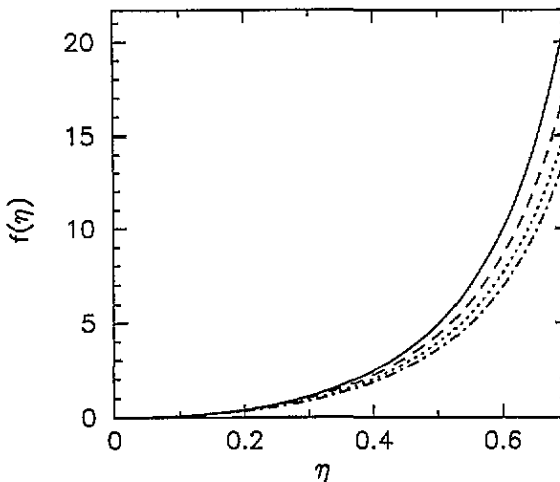


Figure 1. Excess free energy per unit volume against packing fraction for square well fluids. From bottom to top:  $\delta/\sigma = 0.03, 0.02, 0.01$ , all for reduced temperature  $t = 1.0$ . The solid curve is the  $t = \infty$  (hard-sphere) result, equation (2.11).

## 2. The system and its fluid phase properties

Following Bolhuis *et al* we consider hard spheres with a square well attraction and take the interparticle interaction of the form

$$v(r) = \begin{cases} \infty & 0 \leq r < \sigma \\ -\varepsilon & \sigma < r < \sigma + \delta \\ 0 & r \geq \sigma + \delta. \end{cases} \quad (2.1)$$

In equation (2.1),  $\sigma$  is the hard-sphere diameter,  $\delta$  the width of the attractive potential, and  $-\varepsilon$  its depth ( $\varepsilon > 0$ ). We are going to deal exclusively with short-range potentials ( $\delta \lesssim 0.05\sigma$ ). For such a case, there exists an analytic (yet approximate) solution of the Percus–Yevick closure for the direct correlation function of the fluid by Nezbeda [10]. Here we reproduce the essential results of this work, and refer the reader to the original paper for details of the method. Defining  $x = r/\sigma$ ,  $\gamma = \delta/\sigma$  and  $t = k_B T/\varepsilon$  (where  $T$  is the temperature and  $k_B$  Boltzmann's constant), the direct correlation function (dcf)  $c(x)$  is found to have the following form:

$$xc(x) = \begin{cases} -\lambda_1 x - 6\eta\lambda_2 x^2 - \frac{1}{2}\lambda_1 x^4 + 12\eta E(1-E)A^2(2\gamma - x)x & 0 \leq x \leq \gamma \\ -\lambda_1 x - 6\eta\lambda_2 x^2 - \frac{1}{2}\lambda_1 x^4 + 12\eta E(1-E)A^2\gamma^2 & \gamma \leq x < 1 \\ (E-1)[A + B(x-1) + C(x-1)^2] & 1 < x < 1 + \gamma \\ 0 & x > 1 + \gamma. \end{cases} \quad (2.2)$$

The parameters in equation (2.2) above are defined as follows:  $\eta = (\pi/6)\rho\sigma^3$  is the packing fraction ( $\rho = N/V$  is the number density of a system of  $N$  particles enclosed in volume  $V$ ), and  $E = \exp(1/t)$ . The other parameters are calculated by solving algebraic equations as follows. Define

$$\alpha = (12\eta)^2 E(1-E)\gamma^2 \quad \beta = 12(1-E)\gamma. \quad (2.3)$$

Then,  $A$  is the smaller of the two roots of the quadratic equation:

$$[3\eta^2\beta\gamma - (1-\eta)^2]E\eta\beta\gamma A^2 + [\eta(1-\eta)\beta - 3\eta^2\beta\gamma - (1-\eta)^2]A + 1 + \frac{\eta}{2} + \frac{\eta(1-3\eta^2+2\eta^3)}{2(1-\eta)^3}\beta\gamma = 0. \quad (2.4)$$

The remaining parameters are determined from  $A$  through the expressions:

$$B = \frac{(1-\eta)[6\beta\eta^2 - 12\eta(1-\eta)]A + 1 + 7\eta + \eta^2}{(1-\eta)[(1-\eta)^2 - 3\beta\gamma\eta^2]} \quad (2.5)$$

$$\lambda_1 = \frac{(1+2\eta)^2}{(1-\eta)^4} - \frac{\alpha A^2}{(1-\eta)^2} + \frac{2\beta\eta(1+2\eta)}{(1-\eta)^3}(A + \gamma B/2) \quad (2.6)$$

$$\lambda_2 = -\frac{(1+\eta/2)^2}{(1-\eta)^4} + \alpha A^2 \frac{(1+\eta/2)}{6\eta(1-\eta)^2} - \frac{\beta(1+7\eta+\eta^2)}{6(1-\eta)^3}(A + \gamma B/2) \quad (2.7)$$

and

$$C = 3\eta\lambda_1 + 6\eta\lambda_2. \quad (2.8)$$

At low temperatures, there exists a region for the packing fraction for which the discriminant of the quadratic equation (2.4) is negative, and thus no real roots can be found. This observation has led Nezbeda to identify that domain with a two-phase liquid–gas coexistence region of the system [10]. However, here we will be dealing with temperatures much higher than the ‘critical temperature’ of this ‘transition’ where real solutions of the quadratic equation always exist. Moreover, a loss of the solution does not conclusively show that a liquid–gas transition indeed takes place, and even if it does when one looks exclusively at the fluid phases, it might still be preempted by the solid gas transition and thus never materialize in practice.

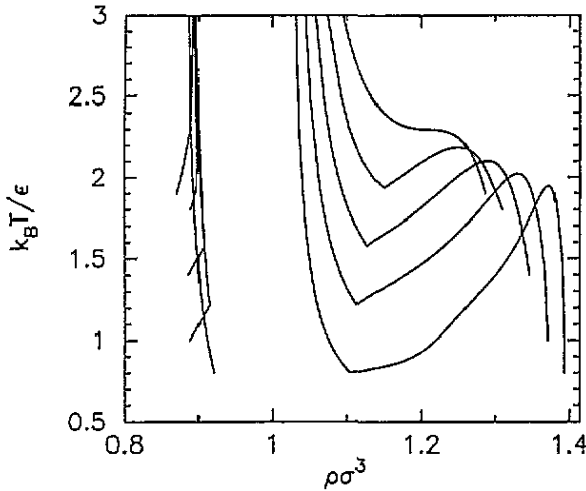


**Figure 2.** Phase diagrams of square well systems obtained using the cMWD. From right to left:  $\delta/\sigma = 0.01, 0.02, 0.03, 0.04$  and  $0.05$ . The bell-shaped curves at high densities give the coexistence between the two fcc solids, with a critical temperature which increases with  $\delta$ . Each such curve continues on the left of the middle density into the solidus curve of the usual melting transition, with the liquidus lines being the leftmost set of curves. The value of  $\delta$  to which the liquidus curves correspond can be identified by the triple temperature, where the slope of the line has a break. For the last value of  $\delta/\sigma$  the fcc–fcc transition is just preempted by melting and thus it never materializes.

From the direct correlation function  $c(x)$ , the equation of state of the system is obtained by means of any of the energy, pressure or compressibility routes. For the MWD which we will apply in this study, it is essential to satisfy the compressibility sum rule. Thus, we choose to obtain the excess free energy of the fluid by invoking this sum rule which relates the  $k = 0$  value of the Fourier transform of the direct correlation function  $c(k)$  to the second density derivative of the excess free energy per unit volume, namely

$$\hat{c}(k = 0; \eta) = -\left(\frac{\pi}{6}\right)^2 f''(\eta) \quad (2.9)$$

where  $\hat{c}(k = 0; \eta) = c(k = 0; \eta)/\sigma^3$  and  $f(\eta) = \beta F_{exc}(\eta)\sigma^3/V$  with  $F_{exc}(\eta)$  being the excess Helmholtz free energy of a system having packing fraction  $\eta$  ( $\beta \equiv (k_B T)^{-1}$  from now on). We integrate numerically equation (2.9) under the initial conditions:

$$f(\eta = 0) = 0 \quad f'(\eta = 0) = 0 \quad (2.10)$$

since both the excess free energy and chemical potential vanish in the ideal ( $\eta \rightarrow 0$ ) limit, to obtain the sought for excess free energy  $f(\eta)$ . In figure 1 we show the excess free

energy of the fluid phase obtained by this procedure for various different values of  $\delta$ . By construction,  $f(\eta)$  reduces at  $t = \infty$  to the 'compressibility free energy'  $f_0(\eta)$  obtained from the Percus–Yevick solution for hard spheres, namely

$$f_0(\eta) = \frac{9}{\pi} \left[ \frac{\eta}{(1-\eta)^2} - \eta \right] - \frac{6}{\pi} \eta \ln(1-\eta). \quad (2.11)$$

Knowing the properties of the uniform fluid, we can now use density functional theory to describe the solid phases and examine their thermodynamic stability.

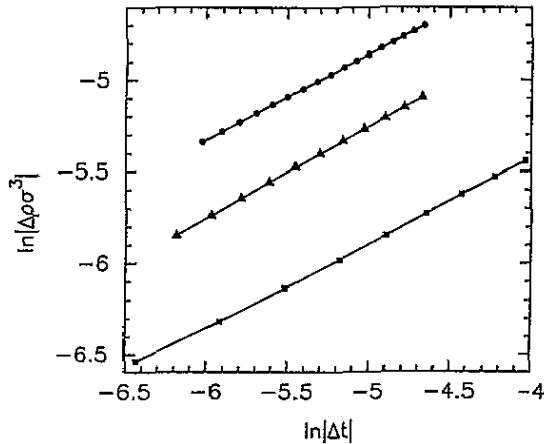


Figure 3. Log-log plot of the deviation of the density from the critical value  $\rho_c$  against the deviation of the temperature from the critical value  $t_c$ . Here  $\Delta\rho\sigma^3 = \rho\sigma^3 - \rho_c\sigma^3$  and  $\Delta t = t - t_c$ . Squares:  $\delta/\sigma = 0.01$ ; triangles:  $\delta/\sigma = 0.02$ ; circles:  $\delta/\sigma = 0.03$ . The straight lines have slopes equal to  $0.5 \pm 0.02$  indicating a value  $\beta = \frac{1}{2}$  for the critical exponent.

### 3. The solid phases

The crystalline solid phases of the system are characterized by a position-dependent one-particle density  $\rho(\mathbf{r})$ . We will therefore refer to the solid as an inhomogeneous (nonuniform) phase, and to the fluid as a homogeneous (uniform) one. According to the basic theorem of density functional theory [11], the Helmholtz free energy of the inhomogeneous system is a *unique functional* of the one-particle density  $\rho(\mathbf{r})$ . This has led to the development of a wide class of different approximations for the study of crystalline solids. Here, we shall adopt the modified weighted density approximation (MWDA) of Denton and Ashcroft [8], which is particularly simple in its implementation, and yet quite successful in its predictions for the freezing of systems characterized by short-range interactions [12]. The basic idea of the MWDA is to first separate the Helmholtz free energy of the solid into an ideal and an excess part:

$$F[\rho] = F_{id}[\rho] + F_{ex}[\rho]. \quad (3.1)$$

The ideal part is known exactly, i.e.

$$\frac{\beta F_{id}[\rho]}{N} = \frac{1}{N} \int \rho(\mathbf{r}) \left[ \ln(\rho(\mathbf{r})\sigma^3) - 1 \right] d\mathbf{r} + 3 \ln(\Lambda/\sigma) \quad (3.2)$$

where  $\Lambda$  is the thermal de Broglie wavelength. On the other hand, the excess free energy is approximated by that of a uniform system evaluated at a weighted density  $\hat{\rho}$ , namely

$$\beta F_{ex}[\rho] = N \tilde{f}(\hat{\rho}) \quad (3.3)$$

with  $N$  the number of particles in the solid and  $\tilde{f}(\rho)$  the excess free energy *per particle* of a uniform system at density  $\rho$ . One may alternatively work with the excess free energy *per unit volume*  $f(\rho) = \rho\sigma^3\tilde{f}(\rho)$  and use

$$\frac{\beta F_{ex}[\rho]\sigma^3}{V} = \rho_s \frac{f(\hat{\rho})}{\hat{\rho}} \quad (3.4)$$

where  $\rho_s = N/V$  is the average density of a solid of  $N$  particles enclosed in volume  $V$ . The weighted density is uniquely specified for a given profile  $\rho(\mathbf{r})$  if the direct correlation function  $c(r)$  and excess free energy  $\tilde{f}(\rho)$  of the uniform system are known [8]. For the density profile, we adopt the usual Gaussian parametrization:

$$\rho(\mathbf{r}) = \left(\frac{\alpha}{\pi}\right)^{3/2} \sum_{\mathbf{R}} \exp\{-\alpha(\mathbf{r} - \mathbf{R})^2\} \quad (3.5)$$

where  $\{\mathbf{R}\}$  is the set of lattice vectors of the given Bravais lattice. Moreover,  $\alpha$  is a localization parameter, and the limit  $\alpha \rightarrow 0$  will be taken to correspond to the uniform fluid, whereas the Gaussians become sharper as  $\alpha$  grows. As a first attempt, we tried to carry out the MWDA mapping (3.3) for the full excess free energy of the solid. However, a problem appears at high solid densities and low temperatures: it turns out that the excess free energy of the solid can become a negative quantity. On the other hand, the excess free energy of the fluid is a nonnegative quantity, for all the values of  $\eta$  and  $t$  that are of interest (see figure 1). Therefore, the mapping cannot *always* be made. To deal with this problem, we first point out that the negative contribution to the solid free energy is entirely due to the 'direct' or 'Hartree' interaction in the solid, defined as

$$F_H[\rho] = \frac{1}{2} \int \int \rho(\mathbf{r})\rho(\mathbf{r}')\phi(|\mathbf{r} - \mathbf{r}'|) d\mathbf{r} d\mathbf{r}' \quad (3.6)$$

where

$$\phi(x) = \begin{cases} -\varepsilon & 1 < x < 1 + \gamma \\ 0 & \text{otherwise} \end{cases} \quad (3.7)$$

is the attractive part of the potential. Thus, we are led to a separation of the Helmholtz free energy of the form

$$F[\rho] = F_{id}[\rho] + F_H[\rho] + F_c[\rho] \quad (3.8)$$

which defines the 'correlation' free energy  $F_c[\rho]$ . We now employ an MWDA-type treatment only for the correlation term, i.e. we write, in analogy with equation (3.4),

$$\frac{\beta F_c[\rho]\sigma^3}{V} = \rho_s \frac{f_c(\hat{\rho})}{\hat{\rho}} \quad (3.9)$$

where  $f_c(\rho)$  is the correlation free energy per unit volume of the uniform system, related to its excess counterpart by

$$f_c(\rho) = f(\rho) - 2\pi(\rho\sigma^3)^2 \int_0^\infty x^2[\beta\phi(x)] dx = f(\rho) + \frac{2\pi(\rho\sigma^3)^2}{3t} [(1 + \gamma)^3 - 1]. \quad (3.10)$$

From equations (3.1), (3.6), (3.8) and the definition of the direct correlation function [11], it follows that

$$\lim_{\rho(\mathbf{r}) \rightarrow \rho} \frac{\delta^2 F_c[\rho]}{\delta\rho(\mathbf{r}) \delta\rho(\mathbf{r}')} = -\beta^{-1} c(|\mathbf{r} - \mathbf{r}'|; \rho) - \phi(|\mathbf{r} - \mathbf{r}'|). \quad (3.11)$$

By defining the 'reduced' direct correlation function  $c_c(|\mathbf{r} - \mathbf{r}'|; \rho)$  as minus  $\beta$  times the left-hand side of (3.11) we obtain

$$c_c(|\mathbf{r} - \mathbf{r}'|; \rho) = c(|\mathbf{r} - \mathbf{r}'|; \rho) + \beta\phi(|\mathbf{r} - \mathbf{r}'|). \tag{3.12}$$

From equations (2.9), (3.9), (3.11) and (3.12) it follows that  $c_c(k = 0; \eta)$  and  $f_c(\eta)$  are related by the 'sum rule'

$$\hat{c}_c(k = 0; \eta) = -\left(\frac{\pi}{6}\right)^2 f_c''(\eta) \tag{3.13}$$

consistently with equation (3.10). The determination of the weighted density  $\hat{\rho}$  appearing in equation (3.9) follows exactly the same steps as the ones in the original MWDA [8], but with the dcf replaced by its reduced counterpart, and the excess free energy by its correlation counterpart. Thus, after some trivial algebra, we find that within the Gaussian parametrization of the solid density, the weighted packing fraction  $\hat{\eta} = (\pi/6)\hat{\rho}\sigma^3$  is given by the self-consistency equation

$$\hat{\eta} = \eta_s \left[ 1 - \frac{18\hat{\eta}^2}{\pi^2(\hat{\eta}f_c'(\hat{\eta}) - f_c(\hat{\eta}))} \sum_{\mathbf{K} \neq \mathbf{0}} e^{-\mathbf{K}^2/2\alpha} \hat{c}_c(\mathbf{K}; \hat{\eta}) \right] \tag{3.14}$$

where  $\eta_s = (\pi/6)\rho_s\sigma^3$  and  $\{\mathbf{K}\}$  is the set of the reciprocal lattice vectors (RLVs) of the given lattice. Alternatively, it turns out to be useful to express the MWDA equation (3.14) in real space, where it reads

$$\hat{\eta} = \eta_s \left[ 1 + \frac{18\hat{\eta}^2 \hat{c}_c(k = 0; \hat{\eta})}{\pi^2(\hat{\eta}f_c'(\hat{\eta}) - f_c(\hat{\eta}))} - \frac{6\hat{\eta}^2}{\pi(\hat{\eta}f_c'(\hat{\eta}) - f_c(\hat{\eta}))} \left( \frac{1}{2N} \int \int \rho(\mathbf{r})\rho(\mathbf{r}')c_c(|\mathbf{r} - \mathbf{r}'|; \hat{\eta}) d\mathbf{r} d\mathbf{r}' \right) \right]. \tag{3.15}$$

Equation (3.15) is more convenient to use for large values of the localization parameter  $\alpha$  ( $\alpha\sigma^2 > 100$ ). Indeed, as the localization grows, one should include more and more stars of RLVs in the  $k$  space iteration (3.14) to ensure the convergence of the sum. However, due to the Gaussian form of the density, and the fact that  $c_c(x)$  has a polynomial form, the integral in (3.15) can be carried out analytically, yielding combinations of powers, exponentials and error functions. Then, one obtains sums over real space stars of lattice vectors, and due to the short-range character of  $c_c(x)$  one only needs to include the  $R = 0$  and the nearest-neighbour contributions to achieve excellent accuracy. A similar treatment can be made for the Hartree term (3.6). There, the analytic expression obtained for  $F_H$  is a lot simpler, and can be found in [5].

**Table 1.** The critical densities  $\rho_c$  of the fcc-fcc transition predicted by simulation, cMWDA and MFA for different values of  $\delta$ .

	$(\rho_c\sigma^3)^a$	$(\rho_c\sigma^3)^b$	$(\rho_c\sigma^3)^c$
$\delta/\sigma = 0.01$	1.374	1.372	1.377
$\delta/\sigma = 0.02$	1.336	1.331	1.340
$\delta/\sigma = 0.03$	1.302	1.290	1.305
$\delta/\sigma = 0.04$	1.267	1.251	1.272

<sup>a</sup> Simulation result ([2]).  
<sup>b</sup> Result from the cMWDA.  
<sup>c</sup> Result from the MFA.



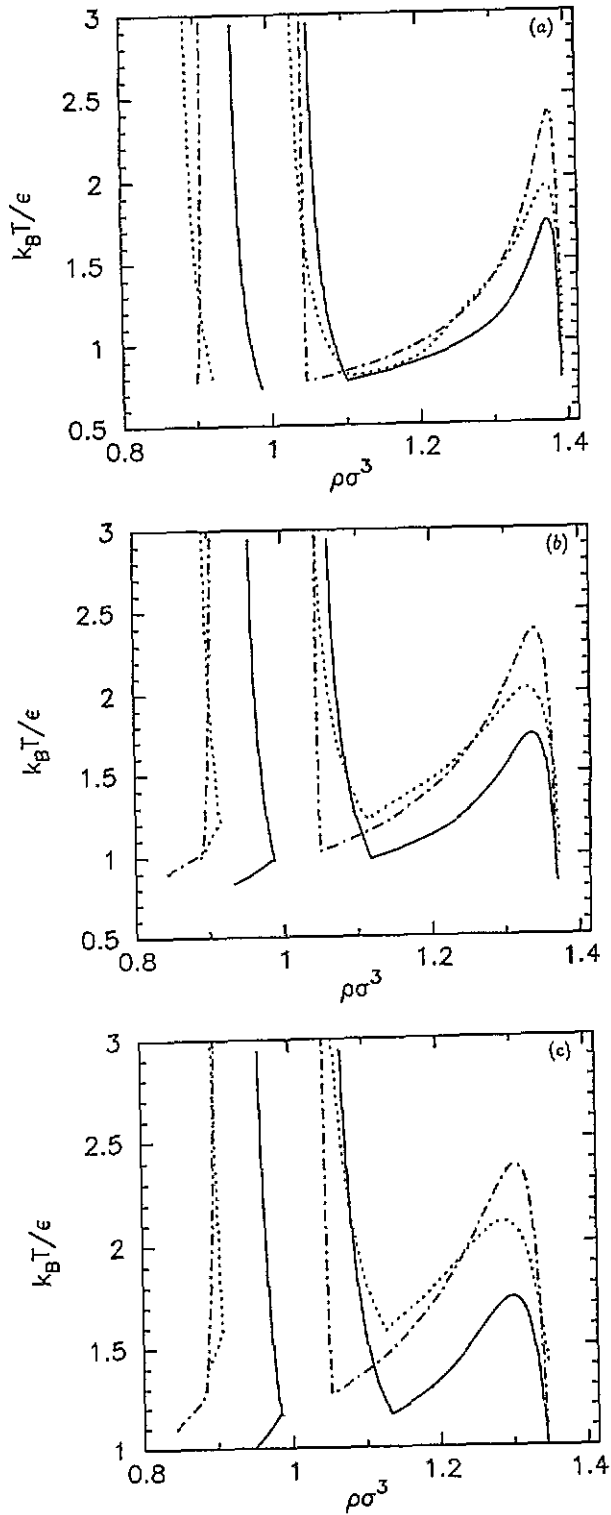


Figure 4. Comparison between simulation, cMWDA and MFA phase diagrams for square well systems. The solid lines are the simulation result, the dotted lines the cMWDA result, and the dash-dotted lines the MFA-result. (a)  $\delta/\sigma = 0.01$ ; (b)  $\delta/\sigma = 0.02$ ; (c)  $\delta/\sigma = 0.03$ ; (d)  $\delta/\sigma = 0.04$ .

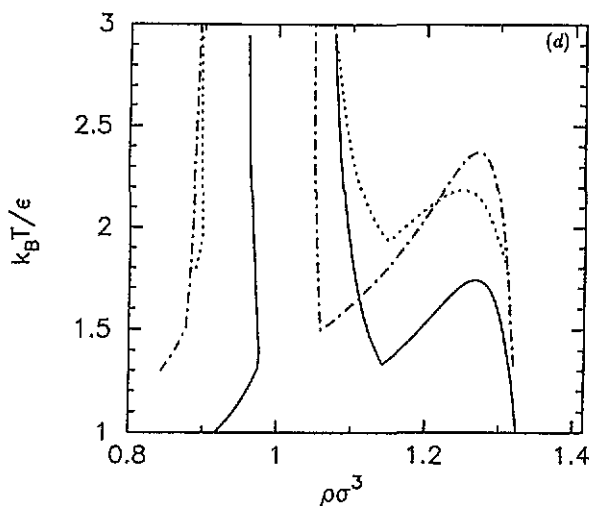


Figure 4. (Continued)

The total free energy of an fcc solid of density  $\rho_s$  is obtained by minimizing the sum of the ideal, Hartree and correlation contributions with respect to the localization parameter  $\alpha$  at fixed  $\rho_s$ . Accordingly, denoting the number density of any phase, solid or liquid by  $\rho$ , we obtain for the Helmholtz free energies per unit volume of our system the following expressions:

$$\begin{aligned}
 f_{sol}(\rho) &\equiv \frac{\beta F_{sol} \sigma^3}{V} \\
 &= \min_{\alpha} \left\{ \rho \sigma^3 \left[ \frac{1}{N} \int \rho(\mathbf{r}) [\ln(\rho(\mathbf{r}) \sigma^3) - 1] d\mathbf{r} \right. \right. \\
 &\quad \left. \left. + \frac{1}{2N} \int \int \rho(\mathbf{r}) \rho(\mathbf{r}') [\beta \phi(|\mathbf{r} - \mathbf{r}'|)] d\mathbf{r} d\mathbf{r}' + \frac{f_c(\hat{\rho} \sigma^3)}{\hat{\rho} \sigma^3} \right] \right\} + 3\rho \sigma^3 \ln(\Lambda/\sigma)
 \end{aligned} \tag{3.16}$$

for the solid and

$$\begin{aligned}
 f_{liq}(\rho) &\equiv \frac{\beta F_{liq} \sigma^3}{V} \\
 &= \rho \sigma^3 (\ln(\rho \sigma^3) - 1) + f_c(\rho \sigma^3) - \frac{2\pi(\rho \sigma^3)^2}{3t} [(1 + \gamma)^3 - 1] + 3\rho \sigma^3 \ln(\Lambda/\sigma)
 \end{aligned} \tag{3.17}$$

for the liquid. The phase diagram is determined by performing the common tangent construction on the solid and liquid free energy curves. In practice the last term in (3.16) and (3.17) is ignored, as it does not affect the location of the phase boundaries. We will refer to this theory as the correlation MWDA (cMWDA).

In order to provide a comparison, we are also going to trace out the phase diagram obtained by treating the system in the mean field approximation (MFA), presented in detail in [7]. The MFA is equivalent to replacing the correlation free energy  $f_c(\rho)$  by the hard-sphere excess free energy, and the reduced correlation function  $c_c(x)$  by the hard-sphere direct correlation function, in all the expressions of this section. To assess the effects of treating the attractive part of the interparticle potential beyond mean-field, we

should compare cMDWA and MFA predictions obtained using liquid inputs of the same quality. In [7], the Carnahan–Starling equation of state [13], and the associated Verlet–Weis parametrization [14] of the direct correlation function were used. Therefore, we recalculate here the MFA phase diagram by using, for the mapping of the solid into an effective liquid, the ‘compressibility’ Percus–Yevick excess free energy  $f_0(\rho)$  (2.11) and the PY dcf  $c_0(x)$  for the hard spheres. (The latter is easily obtained as the  $t = \infty$  or  $\gamma = 0$  limit of the expressions in section 2.) For the liquid free energy  $f_{liq}(\rho)$ , however, we still use in the MFA the more accurate Carnahan–Starling equation, namely

$$f_0^{CS}(\eta) = \frac{6}{\pi} \frac{\eta^2(4 - 3\eta)}{(1 - \eta)^2}. \quad (3.18)$$

The results from both approaches and the comparison with the simulations are presented in the following section.

#### 4. Results and discussion

The phase diagrams obtained using the cMWDA approach are reported in figure 2. We find that there exists a region where two fcc solid phases are separated by a first-order transition region, the region shrinking to a critical point as the temperature is raised, in qualitative agreement with the findings of simulations [2]. This isostructural transition occurs for values  $\delta/\sigma \lesssim 0.05$ ; for larger values of this parameter it is preempted by melting. Moreover, we have also calculated the critical exponent  $\beta$  for the solid–solid transition, finding once more the classical value  $\beta = \frac{1}{2}$  (see figure 3.)

Table 2. The critical temperatures  $t_c$  of the fcc–fcc transition predicted by simulation, cMWDA and MFA for different values of  $\delta$ .

	$(k_B T_c/\epsilon)^a$	$(k_B T_c/\epsilon)^b$	$(k_B T_c/\epsilon)^c$
$\delta/\sigma = 0.01$	1.736	1.945	2.386
$\delta/\sigma = 0.02$	1.736	2.021	2.377
$\delta/\sigma = 0.03$	1.736	2.100	2.372
$\delta/\sigma = 0.04$	1.739	2.186	2.370

<sup>a,b,c</sup> Same as in table 1.

Table 3. The triple temperatures  $t_t$  of the fluid–fcc–fcc coexistence predicted by simulation, cMWDA and MFA for different values of  $\delta$ .

	$(k_B T_t/\epsilon)^a$	$(k_B T_t/\epsilon)^b$	$(k_B T_t/\epsilon)^c$
$\delta/\sigma = 0.01$	0.769	0.800	0.778
$\delta/\sigma = 0.02$	0.980	1.221	1.031
$\delta/\sigma = 0.03$	1.163	1.576	1.268
$\delta/\sigma = 0.04$	1.361	1.935	1.496

<sup>a,b,c</sup> Same as in table 1.

A comparison between simulation, cMWDA and MFA results is presented in figures 4(a)–(d), and the critical densities as well as critical and triple temperatures from theory and simulation are summarized in tables 1–3. The following remarks can be made. First, the critical density is rather insensitive to the particular approximation used, and always in

good agreement with simulation (see table 1). Further, the cMWDA yields better critical temperatures for the fcc–fcc transition as compared with the MFA, which overestimates  $t_c$  by about 37% for all values of  $\delta/\sigma$ . This effect is expected, since in the new theory the correlations between the particles are taken into account in a more accurate way. Nevertheless, the cMWDA still overestimates the critical temperatures by amounts ranging from 12% to 26% depending on the value of the width of the potential (see table 2.) Moreover, the shape of the liquid–fcc coexistence curves (the freezing transition) is better in the new theory: both the liquidus and solidus curves have negative slopes with temperature, whereas in the MFA these curves are almost vertical, with the liquidus curve having slightly positive, and the solidus curve slightly negative slopes. The *width* of the liquid–solid coexistence region is significantly overestimated by the present theory, though. This effect can be understood by noting that this width is largely determined by that of the pure hard-sphere coexistence region, which is the  $t = \infty$  limit of the liquidus and solidus curves. Indeed, for this purely entropic transition, which essentially drives the freezing transition of the system at all temperatures, the MWDA coexistence densities for PY input for both the liquid and solid phases are  $\rho_l\sigma^3 = 0.877$  and  $\rho_s\sigma^3 = 1.018$ , to be compared with  $\rho_l\sigma^3 = 0.940$  and  $\rho_s\sigma^3 = 1.040$  from simulations [15].

At first sight, the new theory appears to be worse than the MFA in two respects. First, the triple temperature  $t_t$  is overestimated with respect to the simulation (see table 3), with the discrepancy between theory and simulation becoming sizeable at larger values of  $\delta/\sigma$ . The MFA also overestimates  $t_t$ , albeit by a smaller amount. Further, the critical temperature  $t_c$  shows a significant dependence on the width of the attractive potential, whereas in both the simulation result and in the MFA  $t_c$  turns out to be quite insensitive to  $\delta$ , being essentially constant. It is not immediately clear at present whether these discrepancies, which increase with  $\delta$ , are due to structural deficiency of the theory itself, or they are consequences of the quality of the liquid state input used in the procedure of mapping the fcc solids onto effective liquids. Nevertheless, a few remarks can be made regarding the possible effects of this liquid input.

From an immediate comparison between the present MFA results and those obtained in [7], where an improved liquid state input was used for the pure hard spheres but the theory was identical otherwise, it can be seen that this input has a significant effect on the estimation of the critical temperature. Indeed,  $t_c$  was found to be equal to about 2.01 before [7], whereas now it turns out to be roughly 2.37, an increase of 18% that can be attributed *entirely* to the liquid state input. Regarding the PY input for the full interaction, there are two factors to be taken into account. First, the analytic solution of Nezbeda [10] is itself approximate, based on an expansion in powers of  $\gamma$  up to  $O(\gamma^2)$  of the direct correlation function  $c(x)$  in the interval  $1 < x < 1 + \gamma$ . The quality of this expansion is bound to get worse as  $\gamma$  increases. In fact, in the original paper [10] results *only* for values  $\gamma \leq 0.01$  are reported, whereas we took here Nezbeda's solution for  $\gamma$  as large as 0.05. Second, even the exact PY solution (obtained by numerically solving the PY equations) has been found to be inaccurate [16] for  $\gamma = 0.5$ . This is of course a value much larger than the ones we consider here, but it would be consistent with a worsening of the PY results as  $\gamma$  grows from zero to higher values.

In this respect, it is interesting to point out that the cMWDA results for the solid–solid transition are in satisfactory agreement with simulation at the smallest value of  $\gamma$ ,  $\gamma = 0.01$ , and worsen systematically as  $\gamma$  grows. It is worth considering, therefore, alternative routes to obtain a more reliable liquid state input, such as the mean spherical approximation for example which has been found to give much better results for large  $\gamma$  [16], or some alternative approaches [17].

## 5. Conclusions

We have presented a density functional approach to study the phase diagram of square well systems with a short-range attraction. So far, the MWDA as well as most of the other approximate density functional schemes have been applied to the freezing in systems interacting by means of simple inverse power potentials. In these cases, the 'phase diagram' consists of just two coexistence densities. On the other hand, in this application the phase diagram is fairly complicated, displaying a nontrivial temperature and interaction dependence, as well as the exciting phenomenon of an isostructural transition. The success of the MWDA in reproducing (at least qualitatively) the simulation results suggests that the theory is capable of dealing with such more complicated situations. However, the lack of a reliable liquid input does not allow at present a definitive assessment of merits and limitations of the MDWA approach. A study of the square well fluid is therefore called for to determine correlation functions and excess free energies of high accuracy, for short-range attraction, say  $0.01 \leq \gamma \leq 0.05$ . Only then will it be possible to settle the issue of the quality of MWDA as well as of any other liquid-based density functional scheme that one might want to apply to this system.

## Acknowledgments

We thank Peter Bolhuis for sending us the simulation results, and Zsolt Németh for helpful discussions. CNL has been supported by the Human Capital and Mobility Programme of the Commission of the European Communities, contract No ERBCHBICT940940.

*Note added in proof.* During the production of this paper, we became aware of another theoretical approach to the problem by Rascón *et al* [18].

## References

- [1] Ilett S M, Orrock A, Poon W C K and Pusey P N 1995 *Phys. Rev. E* **51** 1344
- [2] Bolhuis P, Hagen M and Frenkel D 1994 *Phys. Rev. E* **50** 4880 and references therein
- [3] Bolhuis P and Frenkel D 1994 *Phys. Rev. Lett.* **72** 2221
- [4] Tejero C F, Daanoun A, Lekkerkerker H N W and Baus M 1994 *Phys. Rev. Lett.* **73** 752
- [5] Tejero C F, Daanoun A, Lekkerkerker H N W and Baus M 1995 *Phys. Rev. E* **51** 558
- [6] Daanoun A, Tejero C F and Baus M 1994 *Phys. Rev. E* **50** 2913
- [7] Likos C N, Németh Zs T and Löwen H 1994 *J. Phys.: Condens. Matter* **6** 10965
- [8] Denton A R and Ashcroft N W 1989 *Phys. Rev. A* **39** 4701
- [9] Curtin W A and Ashcroft N W 1986 *Phys. Rev. Lett.* **56** 2775
- [10] Nezbeda I 1977 *Czech. J. Phys.* **B 27** 247
- [11] Evans R 1979 *Adv. Phys.* **28** 143; 1992 *Fundamentals of Inhomogeneous Fluids* ed D Henderson (New York: Dekker) ch 3
- [12] Haymet A D J 1992 *Fundamentals of Inhomogeneous Fluids* ed D Henderson (New York: Dekker) ch 10
- [13] Carnahan N F and Starling K E 1969 *J. Chem. Phys.* **51** 635
- [14] Verlet L and Weis J J 1972 *Phys. Rev. A* **45** 939
- [15] Hoover W G and Ree F H 1968 *J. Chem. Phys.* **49** 3609  
The same values are found in the high-temperature limit of the simulations reported in [2] (Bolhuis P Private communication).
- [16] Smith W R, Henderson D and Tago Y 1977 *J. Chem. Phys.* **67** 5308
- [17] For a discussion on the quality of various liquid state theories for systems with an attractive interaction, see Hansen J P and MacDonald I R 1986 *Theory of Simple Liquids* 2nd edn (New York: Academic) chs 5, 6
- [18] Rascón C, Navasqués G and Mederos L 1995 *Phys. Rev. B* **51** 14 899